SIMULATION OF SOLAR-INDUCED VENTILATION

H B Awbi and G Gan

Department of Construction Management & Engineering
University of Reading, UK

ABSTRACT

Computational fluid dynamics (CFD) is used to simulate the air flow and heat transfer in a Trombe wall and a solar chimney. The CFD results are compared with calculations using heat transfer and fluid flow equations for a closed channel with good agreement.

KEYWORDS

Passive ventilation, computational fluid dynamics, computer simulation, solar air collectors, solar chimneys.

INTRODUCTION

The information technology revolution of the 1980's and the tendency to build deep-plan office buildings have attributed to large increases in internal heat production in commercial buildings. As a result, there has been a vast expansion in the use of airconditioning systems to control the internal environment of such buildings. Although the expansion in the use of refrigeration systems to cool buildings is expected to continue for sometime yet, in the long term buildings will have to rely more on passive ventilation for cooling and fresh air provision. The forthcoming restriction on the use of CFC gases for refrigeration and the production of CO_2, which is a major gas contributing to the greenhouse effect, will inspire designers to apply more passive means for controlling the indoor environment.

Passive ventilation for commercial buildings has not been popular in the past mainly due to the following reasons:

(i) Outdoor air is usually only accessible to perimeter zones of about 6m from windows or ventilation openings.

(ii) The control of ventilation rates is difficult because the air flow is largely influenced by external environmental conditions.

(iii) Because of the lack of control, the energy consumption can be greater than for mechanical ventilation systems and thermal comfort could also be more difficult to achieve.

(iv) Supply of clean outdoor air may be difficult in air-polluted cities.

Most of these problems, real as they are, could be overcome by more intelligent designs and by advanced control systems which are now available at low cost. Even some ancient buildings were passively ventilated using ingenious methods of harnessing and controlling the air flow into the building (Bahadori, 1979).

Most natural ventilation systems rely on wind and buoyancy forces to create the necessary air motion through the building. However, in the absence of wind, buoyancy alone may not be sufficient to provide the required air flow rates. However, by heating the building fabric using solar irradiance it will be possible to enhance the influence of buoyancy as the temperature difference between fabric and air increases. The Trombe wall (Trombe, et al, 1977) and the solar chimney (Bouchair, et al, 1988) have been shown to be effective methods of increasing buoyancy. Both of these systems use vertical solar collectors which are more effective at lower solar altitudes which would occur in arid locations in most seasons, except the summer, and in temperate regions for most of the year.

The performance of the Trombe wall as an air collector has been studied over long periods to predict overall performance (e.g. Sweeney and Wormald, 1988) and over short periods to determine the heat transfer characteristics of the collector (e.g. Akberzadeh et al. 1982). Simulations of the heat conduction in the absorber wall have also been carried out using a numerical solution of the conduction equation to optimize the wall thickness for the storage and emission of heat (e.g. Sweeney and Wormald, 1988). The flow and heat convection in the air gap has been simulated (Borgers and Akbari, 1984) by solving the momentum and energy equations using a finite difference method and the mixing length turbulence model.

In this paper, a computational fluid dynamics (CFD) program developed by the authors is used to simulate the air flow and heat transfer in a Trombe wall for heating the outside air required for ventilation in winter and for inducing ventilation in summer. The flow in a solar chimney is also simulated for summer ventilation. The CFD results are compared with calculations using heat transfer and flow equations for a closed channel. Considering the simplifying assumptions made in the empirical solutions the agreement with the CFD results is generally good.

AIR COLLECTOR PERFORMANCE

The performance of an air collector for the ventilation of a building is assessed by the air flow rate that can be provided, the air supply temperature to the building and the diurnal and seasonal variations of these quantities. These performance parameters can be evaluated using either simple heat transfer and air flow expressions and empirical data or a full CFD simulation of the flow. Both of these techniques are considered here and the results obtained from them are compared in the next section.

Simplified Analytical Approach

Considering buoyancy effects only (i.e. excluding wind effects) the volume of air flow rate, V (m^3/s), produced by a vertical air collector is given by:

$$V = (C_d\ A)_e \sqrt{4gH\ \left(\frac{T_m - T_i}{T_m}\right)} \qquad (1)$$

where T_i and T_m are the inlet and mean air temperatures of the collector (K), H is the height between inlet and outlet openings and $(C_d\ A)_e$ is the product of effective discharge coefficient and area of the collector openings, Fig. 5(a). This is given by:

$$(C_d\ A)_e = \sum_{i=1}^{n} (C_d\ A)_i \qquad (2)$$

for openings in parallel, and

$$\frac{1}{(C_d\ A)_e^{\,2}} = \sum_{i=1}^{n} \frac{1}{(C_d\ A)_i^{\,2}} \qquad (3)$$

for openings in series, where n is the number of openings.

The pressure losses in the collector can be evaluated using:

$$\Delta P = \left[\ 4f\ \frac{H}{D_h} + K_i\ \left(\frac{A_m}{A_i}\right)^2 + K_d\ \left(\frac{A_m}{A_d}\right)^2 + K_o\ \left(\frac{A_m}{A_o}\right)^2\ \right] \tfrac{1}{2}\rho_m V_m^{\,2} \qquad (4)$$

where the K's are the pressure loss coefficients, the A's are the flow areas, H is the height between the top and bottom openings, ρ is the air density and V is the mean velocity. Subscripts i, d, o and m refer to inlet, damper (or other fittings), outlet and channel respectively. The hydraulic diameter of the channel, D_h, is given by:

$$D_h = \frac{2\ W\ h}{W + h} \qquad (5)$$

where W is the channel width and h is the distance between the two walls. For a narrow channel (i.e. W >> h) $D_h \approx 2h$.

The convective heat transfer between the collector surface and air is given by:

$$Q = h_c\ A\ (T_w - T_{ai}) \qquad (6)$$

where h_c is the convective heat transfer coefficient, A is the surface area and T_w and T_{ai} are the temperatures of wall and inlet air. The heat transfer coefficient h_c can be evaluated using:

$$Nu = 0.09\ Ra^{1/3} \qquad (7)$$

for turbulent flow ($10^{13} > Ra > 10^9$), and

$$Nu = 0.53\ Ra^{1/4} \qquad (8)$$

for laminar flow ($10^9 > Ra > 10^4$). The Nusselt number Nu and the Rayleigh number Ra are given by:

$$Nu = h_c\ y/k$$

$$Ra = Pr\ Gr$$

where $Pr = \mu C_p/k$ = Prandtl's number

$Gr = g\beta y^3(T_w - T_{ai})/\upsilon^2$ = Grashof's number

The air temperature in the collector at any height y above the inlet is obtained from:

$$T_a = A/B + (T_{ai} - A/B)\ \exp(-B\ W\ y/\dot{m}C_p) \qquad (9)$$

where $A = h_w T_w + h_g T_g$

$B = h_w + h_g$

and subscripts w and g refer to wall and glazing (as in a Trombe wall), T_{ai} is the inlet air temperature and $\dot{m}$ is the mass flow rate of air in the collector. For heat transfer from one surface only, equation (9) reduces to:

$$T_a = T_w + (T_{ai} - T_w)\ \exp(-h_w\ W\ y/\dot{m}C_p) \qquad (10)$$

Further details are given in Appendices (A) and (B).

CFD SOLUTION

The analysis given earlier can be used for the sizing of vertical air collectors but does not provide information on the air flow patterns in the collector or the building which it serves. The latter requires the application of a computational fluid dynamics (CFD) program.

Here, a CFD program developed by the authors is used for predicting the air flow within the collector and the ventilated space. The program is a three-dimensional finite volume code which uses the k-ϵ turbulence model and solves the Navier-Stokes

equations, the energy equation and the equations for the turbulence energy (k) and its dissipation (ϵ). These equations have the general form:

$$\frac{\partial}{\partial x_i}(\rho U_i \phi) = \frac{\partial}{\partial x_i}(\Gamma_\phi \frac{\partial \phi}{\partial x_i}) + S_\phi \qquad (11)$$

convection diffusion source

where the dependent variable ϕ represents the velocity components U, V and W, the temperature T, the turbulence scales k and ϵ and Γ_ϕ is the difusion coeficient. The source term S_ϕ is given by different expressions for each ϕ. A staggered grid is used for solving the equations using the SIMPLE pressure correction procedure. At solid boundaries wall function expressions are used for the first grid point from the boundary. The iterative solution procedure is repeated until a converged solution is achieved (Awbi, 1991, Awbi and Gan, 1991).

When a CFD program is used for predicting buoyancy-driven flows it is necessary to know the pressure difference between the air inlet and outlet openings which is required for Bernoulli's equation to specify the air flow rate into the system. Equation (1) is used to calculate the flow into the collector for every iteration.

RESULTS AND DISCUSSION

Trombe Wall

Trombe wall collectors have traditionally been used for space heating by allowing air from the room to enter near the bottom of the wall which is heated by the collector and then returned back to the room at high level. This does not normally include fresh air supply to the room and assumes that fresh air is provided fortuitously by air infiltration through the building fabric. However, as modern methods of construction produce tighter building fabric attention should be directed towards controllable provision of fresh air to the building. A Trombe wall collector is a passive ventilator which can provide means of controlling the air flow using dampers. The performance of a Trombe wall collector as a passive ventilator is demonstrated here for winter and summer situations.

A room 5m long x 3.4m wide x 2.8m high is used in this study. A collector wall of thickness 0.3m having the same width and height as the room is situated at one end of the room. The distance between the wall and the glazing is 0.1m. When the outside air requires heating the air enters through an external slot 1.2m x 0.1m at a height of 0.2m from the floor and leaves through two slots o.6m x 0.1m each at a height of 2.5m from the floor. If the outside air is supplied directly into the room it enters through a window on a wall opposite the collector and enters the bottom of the collector through two 0.6m x 0.1m slots open to the room, and leaves at the top of the collector through a single 1.2m x 0.1m slot.

The results of the CFD simulations are compared with those calculated using equations (1) and (10) in Table 1 and Figure 1.

Table 1 Calculated and simulated flow rates for a Trombe wall

Case	Gr_H^*	T_{ai} (°C)	T_w (°C)	T_g (°C)	Outlet temp (°C)		Flow rate (m^3/s)	
					Calculated	Simulated	Calculated	Simulated
1	4.0×10^{10}	10.0	30	10	14.2	15.6	0.080	0.088
2	2.8×10^{10}	15.0	30	20	18.6	20.0	0.075	0.078
3	5.0×10^{10}	22.6	50	20	28.7	28.0	0.091	0.110

* Gr_H is based on $(T_w - T_{ai})$ and H

The air flow rates and the exit temperatures from the collector obtained using the two methods are reasonably close. According to ventilation guides (e.g. ASHRAE Standard 62-89, CIBSE) these flow rates should provide sufficient fresh air for about 10 occupants. The increase in the bulk air temperature with height is shown in Fig.1. Although the two procedures show similar temperature profiles there is some difference particularly near the outlet from the collector. This discrepancy is to be expected since the analytical method assumes a two-dimensional flow between two parallel surfaces and does not take into consideration the disturbance to the flow caused by the inlet and outlet openings of the collector. The turbulence generated by the inlet openings could produce a fully turbulent flow throughout the collector and causes the flow to be three-dimensional as it expands into the gap between the two collector surfaces.

The air flow patterns in the collector and room obtained from the three CFD simulations can be seen in Figs. 2 to 4. The object in the middle of the room represents a person, including the heat output, with all internal room surfaces assumed to be adiabatic. When the outside temperature is low (10°C), cold draught is present in the room (Fig. 2) which is caused by the two cold jets dropping into the room (dumping). With higher outdoor temperature (15°C) the air movement in the room becomes acceptable as depicted by Fig. 3. Therefore, additional heating will be needed to improve the conditions in the room with outdoor air temperature of 10°C or lower for a collector wall temperature of 30°C. The cooling of the room by inducing outdoor air through the window is shown in Fig. 4. The air jet drops onto the floor thus cooling and ventilating the occupied zone in a warm climate. There is clearly long wave radiation from the collector wall which could increase the room temperature in the summer. However, this can be reduced by internally insulating the wall.

Solar Chimney

A solar chimney added to the south or south west wall of a building can be heated by solar energy and the heat stored in its fabric is then utilised for ventilation by opening dampers as shown in Fig. 5(b).

The purpose of the chimney is to provide passive ventilation and

also cooling in hot climates. By opening a window or other openings air will be drawn into the room from outside which then enters the chimney through the lower opening where it is heated and then exhausted. Given sufficient solar energy a solar chimney could provide sufficient ventilation for most of the day (Bouchair et al, 1988). If the spacing between the chimney walls is of the same order as for a Trombe wall then the same analysis can be applied for predicting the ventilation performance of the chimney where in this case the collector wall is outside. If the spacing is too large then this type of analysis may be inherently less accurate because of the large variation in air velocity and temperature across the gap. In this case a CFD simulation will provide the necessary performance data.

The flow in the chimney which was investigated experimentally by Bouchair et al has been simulated using CFD. The chimney's height, H, is 1.95m, the width, W, is 1.5m and the distance between the two walls, h, is 0.3m. The inlet opening is 1.2m wide and 0.1m high and it is located 0.1m above the floor. The effect of chimney wall temperature on the air flow rate through the chimney is shown in Fig. 6 in which case both walls are heated to the same temperature. Although in practice the two chimney walls are not expected to be at the same temperature the simulation was performed to provide a comparison with the laboratory measurements of Bouchair at al. The experimental data shows that the air flow rate increases steeply as T_w increases further. The difference between prediction at T_w = 50°C and measurement is about 14%. A simulation with only one wall heated produced a flow rate of almost half that for two heated walls.

The simulated air velocity and temperature distributions across the solar chimney at its exit are shown in Fig. 7. Because the air enters the chimney at right angle to its axis these profiles are not symmetrical. A simulation was carried out with air entering axially which produced symmetrical profiles about the axis. The velocity profile for the chimney with two heated walls show two velocity peaks due to the two thermal boundary layers. The profile with one heated wall produces peak velocities away from the heated wall. The velocity vectors and temperature contours for these two cases are shown in Fig. 8.

CONCLUSIONS

Solar-induced ventilation could be effective in using buoyancy to provide airtight buildings with sufficient fresh air. A Trombe wall collector can be used to heat the air before it enters the occupied space in winter and it can also be used to create air movement in the occupied space for cooling in the summer. A solar chimney is more suitable for summer ventilation in hot climates. It has been shown that the design of these air collectors can be carried out with reasonable accuracy by applying standard heat transfer and fluid flow formulae but to study the air movement in detail a CFD simulation is needed. In particular a CFD simulation provides qualitative and quantitative design information on the air movement in the collector and in the space to which air is supplied.

REFERENCES

Akbarzadeh, A., et al. (1982). Thermocirculation characteristics of a Trombe wall passive test cell. **Solar Energy, 28**, pp 461-468.

Awbi, H.B., (1991). **Ventilation of Buildings**, Spon, London.

Awbi, H.B., and Gan, G., (1991). Computational fluid dynamics in ventilation. **Proc. CFD for Environmental and Building Services Engineer**, Institution of Mechanical Engineers, London.

Bahadori, M.N. (1979). Natural cooling in hot arid regions. In: **Solar Energy Application in Buildings** (A.A.M. Sayigh, ed.) chapter 9, pp 195-225, Academic Press, New York.

Borgers, T.R. & Akbari, H. (1984). Free convective turbulent flow within the Trombe wall channel. **Solar energy, 33**, pp 253 - 264.

Bouchair, A., et al. (1998). Moving air, using stored solar energy. In: **Proc. 13th National Passive Solar Conference**, Cambridge, Massachusettes.

Holman, J.P. (1990). **Heat Transfer**, Chapter 7, pp 340 - 343, McGraw-Hill, New York.

Sweeney, M.E. and Wormald, R. (1998). Monitoring, computer simulation and improvement of the performance of a fan assisted solar wall. In: **Advances in Solar Energy Technology** (W.H. Bloss and F. Pfisterer, eds.), Vol. 4, pp 3642 - 3646, Pergamon Press, Oxford.

Trombe, F. et al (1977). Concrete walls to collect and hold heat. **Solar Age, 2**, 13 - 35.

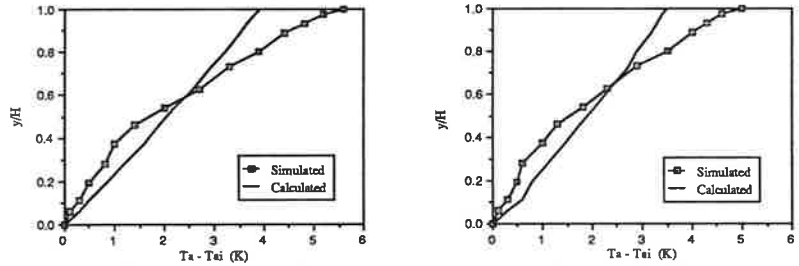

(a) Heating with Tai = 10 deg.C

(b) Heating with Tai = 15 deg.C

(c) Ventilation with Tai = 22.6 deg.C

Fig. 1 Trombe wall air temperature

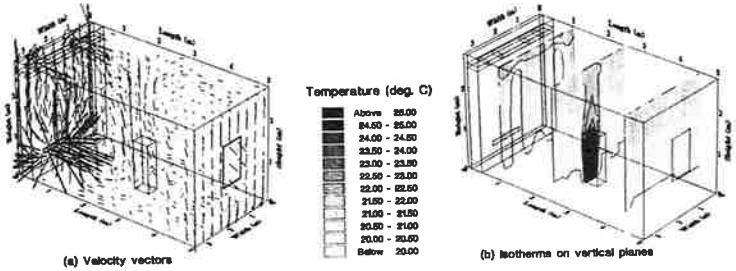

Fig. 2 Predicted velocity vectors and isotherms in a naturally ventilated room with a Trombe wall for heating
Temperatures (deg.C): outdoor air = 10 ; Trombe wall = 30

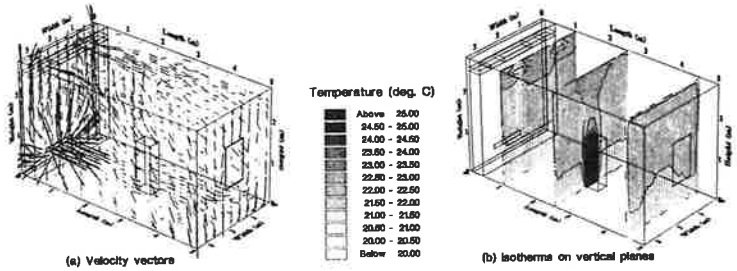

Fig. 3 Predicted velocity vectors and isotherms in a naturally ventilated room with a Trombe wall for heating
Temperatures (deg.C): outdoor air = 15 ; Trombe wall = 30

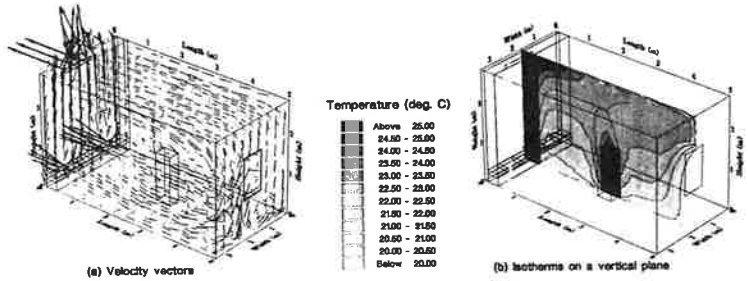

Fig. 4 Predicted velocity vectors and isotherms in a naturally ventilated room with a Trombe wall
Temperatures (deg.C): outdoor air = 20 ; Trombe wall = 50

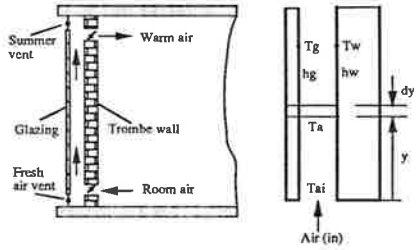

Fig. 5(a) Trombe wall

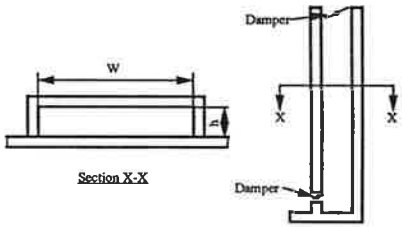

Fig. 5 (b) Solar chimney

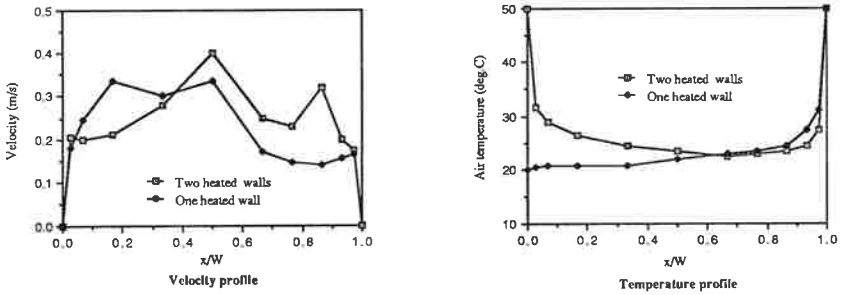

Fig. 7 Velocity and temperature profiles at the exit from a solar chimney

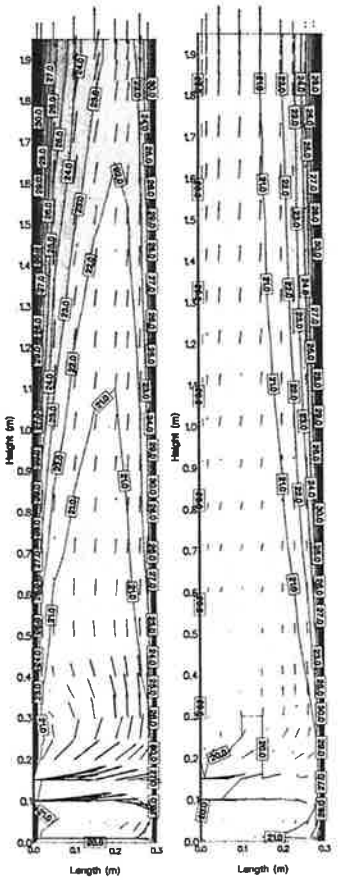

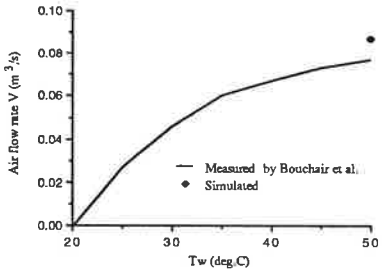

Fig. 6 Effect of chimney wall temperature on the flow rate

Fig. 8 Predicted velocity vectors and isotherms in a solar chimney

Left: two heated walls
Right: one heated wall

Temperature: inlet air = 20°C
heated wall = 50°C
unheated wall = 20°C

Velocity scale : 1 m/s ⟶

APPENDIX (A)

AIR FLOW IN COLLECTOR

Buoyancy Equation

The buoyancy (stack) pressure, p, at a point distance y above a datum is:

$$p = p_o - \rho g y \qquad (A.1)$$

where p_o is the datum pressure (Pa) and ρ is the air density (kg/m^3). The pressure difference, dp, between two points separated by a vertical displacement dy is:

$$dp = -\rho p g \, dy = -\rho_o g \, T_o/T \, dy \qquad (A.2)$$

where ρ_o is the air density at a reference temperature T_o (K) and T is the air temperature (K).

Integrating Equation (A.2) gives the pressure difference, Δp, between the lower and upper openings of the wall shown in Fig. 5(a):

$$\Delta p = \rho_o \, T_o \, g \, H \left(\frac{1}{T_i} - \frac{1}{T_e} \right) \qquad (A.3)$$

where H is the vertical spacing of the two openings (m) and T_i and T_e are the air temperatures at either side of the openings.

The air volume flow rate, $\dot{V}$, through the two openings is:

$$\dot{V} = (C_d \, A)_e \sqrt{(2\Delta p/\rho_o)} \qquad (A.4)$$

where $(C_d \, A)_e$ is the product of effective discharge coefficient and area of the flow openings. Substituting for Δp from Equation (A.3) and taking the reference temperature as $T_o = T_m = \frac{1}{2}(T_i + T_e)$, we find that:

$$\dot{V} = (C_d \, A)_e \sqrt{2gH \, T_m \left(\frac{1}{T_i} - \frac{1}{T_e} \right)} \qquad (A.5)$$

In Equations (A.4) and (A.5) the pressure loss in the gap between the two surfaces has been ignored because this is usually small in comparison with the pressure loss at the inlet and outlet (Trombe, et al., 1977). In the case of the collector shown in Fig. 5(a) the air temperature over the collector surface varies between the inlet temperature, T_i, and the exit temperature, T_e. Defining the mean temperature as $T_m = \frac{1}{2}(T_i + T_e)$ then $T_e = 2T_m - T_i$. Substituting for T_e in Equation (A.5) and assuming that $T_m^2 \approx T_i T_e$ Equation (A.5) becomes:

$$\dot{V} = (C_d \, A)_e \sqrt{4gH \left(\frac{T_m - T_i}{T_m} \right)} \qquad (A.6)$$

The evaluation of $(C_d\ A)_e$ in Equation (A.6) depends on whether the openings are connected in series or in parallel. For openings in parallel (i.e. flow entering or leaving all the openings) the pressure difference across each opening should be the same and the total flow rate is the sum of the flow rates through each opening. Hence, from Equation (A.4) for openings in parallel:

$$(C_d\ A)_e = \sum_{i=1}^{n} (C_d\ A)_i \qquad (A.7)$$

where n is the number of openings.

For openings in series (i.e. the same flow entering one opening and leaving through another opening) the flow rate through each opening is the same but the pressure difference across the openings is the sum of the pressure difference across each opening. Hence, from Equation (A.4) for openings in series:

$$\frac{1}{(C_d\ A)_e^2} = \sum_{i=1}^{n} \frac{1}{(C_d\ A)_i^2} \qquad (A.8)$$

Pressure Losses

For an air collector the buoyancy pressure must equal to the sum of all the pressure losses as a result of the air flow. The pressure losses are at the inlet and outlet openings of the channel, across fittings such as dampers, and fluid friction at the channel walls. Therefore, the total pressure loss ΔP is:

$$\Delta P = \Delta P_i + \Delta P_d + \Delta P_f + \Delta P_o \qquad (A.9)$$

where $\Delta P_i = K_i\ \frac{1}{2}\rho_i V_i^2$ = pressure loss at inlet opening

$\Delta P_d = K_d\ \frac{1}{2}\rho_d V_d^2$ = pressure loss across a damper

$\Delta P_o = K_o\ \frac{1}{2}\rho_o V_o^2$ = pressure loss at outlet opening

$\Delta P_f = 4f\ H/D_h\ \frac{1}{2}\rho_m V_m^2$ = pressure loss in duct due to friction.

In the above expressions K is the pressure loss coefficient, ρ is the local air density, V is a reference velocity, ρ_m and V_m are mean values for the duct, f is the friction factor, H is the height (length) of duct and the hydraulic diameter, D_h, is given by:

$$D_h = \frac{2\ W\ h}{W + h} \qquad (A.10)$$

where W is the width of duct section and h is the distance between the two duct walls. For a narrow channel (e.g. Trombe collector), $D_h \approx 2h$.

Assuming that density variations are small, Equation (A.9) may be written in terms of mean channel velocity as:

$$\Delta P = \left[4f\ \frac{H}{D_h} + K_i \left(\frac{A_m}{A_i}\right)^2 + K_d \left(\frac{A_m}{A_d}\right)^2 + K_o \left(\frac{A_m}{A_o}\right)^2 \right] \frac{1}{2}\rho_m V_m^2 \qquad (A.11)$$

where the area ratios represent the mean duct area, A_m, to the opening area.

APPENDIX (B)

HEAT TRANSFER IN COLLECTOR

Convection Heat Transfer Coefficient

The convective heat transfer between a surface at temperature T_w and air at a bulk temperature T_{ai} is:

$$Q = h_c\ A\ (T_w - T_{ai}) \qquad (B.1)$$

where h_c is the surface heat transfer coefficient and A is the surface area. For turbulent flow involving a vertical wall h_c can be obtained from an expression such as (Holman, 1990):

$$Nu = 0.1\ Ra^{1/3} \qquad (B.2)$$

for $10^{13} > Ra > 10^9$. In this equation:

$Nu = h_c\ y/k$ = Nusselt's number

$Ra = Pr\ Gr$ = Rayleigh's number

$Pr = \mu C_p/k$ = Prandtl's number

$Gr = g\beta y^3(T_w - T_{ai})/\upsilon^2$ = Grashof's number

In a Trombe wall channel it has been found (Akbarzadeh at al. 1982) that Equation (B.2) overestimates h_c by about 10% and a better correlation with measurements was achieved using:

$$Nu = 0.09\ Ra^{1/3} \qquad (B.3)$$

For laminar flow ($10^9 > Ra > 10^4$) Holman (1990) gives the expression:

$$Nu = 0.59\ Ra^{1/4} \qquad (B.4)$$

In the case of a Trombe wall channel and assuming that Equation (B.4) overestimates h_c also by 10% the equation for laminar flow becomes:

$$Nu = 0.53\ Ra^{1/4} \qquad (B.5)$$

When convective heat transfer occurs on the two surfaces of a channel Equations (B.3) and (B.5) are applied to each surface to obtain the heat transfer coefficient for the two surfaces. In this case T_w represents the temperature of the wall and T_{ai} is the

inlet air temperature to the channel.

Air Temperature in Collector

The increase in air temperature of the collector is due to heat transfer by convection from the wall and glazing surfaces. For an element of thickness dy at a height y from the collector base an energy balance gives (see Fig. 5(a)):

$$\frac{\dot{m}}{W} C_p \frac{\partial T_a}{\partial y} = h_w (T_w - T_a) + h_g (T_g - T_a) \qquad (B.6)$$

Where $\dot{m}$ is the mass flow rate of air (kg/s), W is the width of collector, C_p is the specific heat of air, T_w and T_g are the wall and glazing temperatures and h_w and h_g are the corresponding heat transfer coefficients. Integrating Equation (B.6) and rearranging, the air temperature at any point in the collector will be given by:

$$T_a = A/B + (T_{ai} - A/B) \exp(-B\ W\ y/\dot{m}C_p) \qquad (B.7)$$

where T_{ai} is the inlet air temperature and A and B are given as:

$$A = h_w T_w + h_g T_g$$

$$B = h_w + h_g$$

If one of the walls (e.g. glazing) is assumed adiabatic, then Equation (B.7) becomes:

$$T_a = T_w + (T_{ai} - T_w) \exp(-h_w\ W\ y/\dot{m}C_p) \qquad (B.8)$$